AIAA JOURNAL
Vol. 31, No. 11, November 1993

Approximate Elasticity Solution for Laminated Anisotropic Finite Cylinders

Hung-Sying Jing* and Kuan-Goang Tzeng†
National Cheng Kung University, Tainan 70101, Taiwan, Republic of China

This paper deals with the static response of the axisymmetric problem of arbitrarily laminated, anisotropic cylindrical shells of finite length using three-dimensional elasticity equations. The closed cylinder is simply supported at both ends. The highly coupled partial differential equations (PDEs) are reduced to ordinary differential equations (ODEs) with variable coefficients by choosing the solution composed of trigonometric functions along the axial direction. Through dividing each layer into thin laminas, the variable coefficients in ODEs become constants, and the resulting equations can be solved exactly. Numerical examples are presented for [−45/0 deg] and [−45/45/−45 deg] laminations under sinusoidal normal loading on the outer surface and uniform internal pressure. From the present study, it is found that, although the general behavior is similar to that of isotropic shells, the coupling is obvious in general, and the shear effect is very important in the edge region. Moreover, the initial curvature effect plays an essential role, especially in stress distributions.

Introduction

STATIC and dynamic responses of composite laminated closed cylindrical shells and curved panels have received wide attention in recent years. Because of the anisotropy in composites and the presence of curvature in shell structures, obtaining exact three-dimensional elasticity solutions for laminated closed cylinders and open panels subjected to general loading and arbitrary boundary conditions becomes a challenging task. The mathematical complexity in analyzing three-dimensional elasticity equations usually makes exact solutions difficult to obtain. However, certain problems in which a three-dimensional approach can be used still exist.

Most of these problems can be solved by assuming the solution to be composed of trigonometric functions in the axial and circumferential directions. The main reason is that the partial differential equations (PDEs) governing three-dimensional problems can be reduced to one-dimensional ordinary differential equations (ODEs) with variable coefficients. The solution for the resulting ODEs can be obtained by introducing the displacement potential function. Usually, this method is used with isotropic and transversely isotropic materials, whereas the Frobenius method is used with orthotropic materials. When the three-dimensional elasticity solutions are available, they are very useful in evaluating the accuracy of approximate results, e.g., in the case of two-dimensional shell theories.

For the static problem, Flugge and Kelkar[1] and Yao[2] obtained an exact solution for closed isotropic long cylinders under general two-dimensional surface traction. Using the Frobenius method, Srinivas[3] developed an exact three-dimensional solution for orthotropic finite cylinders with simply supported conditions. However, the numerical results are given for free vibration only. Varadan and Bhaskar[4] also performed the static stress analysis using the procedures proposed by Srinivas. Pagano[5] obtained the stress field for a homogeneous, anisotropic closed cylinder under two-dimensional surface loads in which the problems are independent of the axial coordinate. However, numerical results are reported only for a single orthotropic layer. Recently, Ren[6,7] presented an exact solution for simply supported laminated cross-ply circular cylindrical panels of infinite and finite length in the axial direction. Mikhailov[8] presented a general solution of the axisymmetrical torsional equation for infinitely long, elastic cylindrically anisotropic shells. The stresses and deformations in cross-ply composite cylinders due to a circumferential temperature gradient in which the problem is independent of the axial coordinate have been analyzed by Hyer and Cooper.[9] An extension was made by Kollar et al.[10] for the generally anisotropic composite cylinders subjected to hygrothermal and mechanical loads. More recently, Huang and Tauchert[11,12] investigated the elastic response of cross-ply cylindrical panels and double-curved shell panels subjected to mechanical loading and temperature variation using a power series method.

Although the aforementioned three-dimensional elasticity approach provides exact solutions, considerable mathematical complexity prevents more general problems from being solved. As a consequence, an approximate elasticity approach under the assumption of $h_k/R_k \ll 1$ (where h_k and R_k denote the thickness and mean radius of the kth lamina) was suggested by Soong[13] and widely used in the static and free vibration analysis of fiber-reinforced composite-laminated closed cylindrical shells and panels.[14-19] The advantage of this assumption is that the ODEs with variable coefficients can be reduced to simple ODEs with constant coefficients that can be solved exactly. Accurate results can be achieved when the number of fictitious layers becomes sufficiently large.

Based on the aforementioned approximate elasticity approach, the static response of simply supported cross-ply laminated cylindrical panels was analyzed by Bhimaraddi and Chandrashekhara.[14] An analytical solution of the axisymmetric problem for interlaminar stresses in cross-ply laminated closed cylinders under thermal and mechanical loads was provided by Wang and Li.[15] Soldatos and Hadjigeorgiou[16] studied the free vibration problem for homogeneous, isotropic closed cylinders and open panels of finite length with simply supported boundary conditions. Extensive work was done by Soldatos[17] on the torsional vibrations of orthotropic closed cylinders. A very good comparison between approximate results and exact elasticity solutions was observed. A solution for the axisymmetric vibration problems of cross-ply laminated closed cylinders was also obtained by Hawkes and Soldatos.[18] Additionally, Bhimaraddi[19] derived the solution for the free vibration problem of homogeneous cross-ply laminated doubly curved shallow shells of rectangular planform.

A brief survey of the literature shows that elasticity solutions to the problem of arbitrarily laminated, anisotropic closed cylinders of finite length have not yet been investigated. Although the solutions from classical shell theory and first-order shear deformation theory are available,[20,21] in this paper a

Received Oct. 15, 1992; revision received March 19, 1993; accepted for publication March 30, 1993.

*Professor, Institute of Aeronautics and Astronautics.
†Graduate Student, Institute of Aeronautics and Astronautics.

solution based on an elasticity equation is presented for the static axisymmetric problem of arbitrarily laminated, anisotropic closed cylindrical shells of finite length with simply supported boundary conditions. The solution is essentially based on the approach proposed by Soong and used by some others as described in the previous paragraph. A general solution of displacements and stresses is obtained. A convergence study is established for a single anisotropic layer [45 deg] under sinusoidal normal loading with two mean-radius-to-thickness ratios, in which the number of fictitious layers ranges from 1 to 20. In the first example, two types of stacking sequence, [− 45/0 deg] and [− 45/45/ − 45 deg], are used. The radial displacement and some of the stresses are listed and compared with classical shell theory. The second example illustrates the behavior of thick shells under uniform internal pressure. Finally, comments are made on general behavior and boundary layer.

Problem Description

Consider a laminated composite closed cylinder made of N perfectly bonded homogeneous anisotropic layers whose principal axes coincide with three orthogonal coordinates r, θ, and x, as shown in Fig. 1. The r, θ, and x represent the radial, circumferential, and axial coordinates. Each layer of the composite has one plane of elastic symmetry perpendicular to the thickness direction (i.e., monoclinic material). The thickness and mean radius of the kth lamina are denoted by h_k and R_k; R_i, R, and R_o are the inner, mean, and outer radii; and h and L stand for the total thickness and length of the cylinder. Having one plane of elastic symmetry, the constitutive equation of each layer in which 13 elastic constants are involved is stated as follows:

$$\begin{Bmatrix} \sigma_x \\ \sigma_\theta \\ \sigma_r \\ \tau_{r\theta} \\ \tau_{xr} \\ \tau_{x\theta} \end{Bmatrix} = \begin{bmatrix} C_{11} & C_{12} & C_{13} & 0 & 0 & C_{16} \\ C_{12} & C_{22} & C_{23} & 0 & 0 & C_{26} \\ C_{13} & C_{23} & C_{33} & 0 & 0 & C_{36} \\ 0 & 0 & 0 & C_{44} & C_{45} & 0 \\ 0 & 0 & 0 & C_{45} & C_{55} & 0 \\ C_{16} & C_{26} & C_{36} & 0 & 0 & C_{66} \end{bmatrix} \begin{Bmatrix} \epsilon_x \\ \epsilon_\theta \\ \epsilon_r \\ \gamma_{r\theta} \\ \gamma_{xr} \\ \gamma_{x\theta} \end{Bmatrix} \tag{1}$$

Since the present study focuses on the axisymmetric problem, the equilibrium equations become

$$\begin{aligned} &\frac{1}{r}\frac{\partial(r\sigma_r)}{\partial r} + \frac{\partial \tau_{xr}}{\partial x} - \frac{\sigma_\theta}{r} = \rho \frac{\partial^2 u_r}{\partial t^2} \\ &\frac{1}{r^2}\frac{\partial(r^2\tau_{r\theta})}{\partial r} + \frac{\partial \tau_{x\theta}}{\partial x} = \rho \frac{\partial^2 u_\theta}{\partial t^2} \\ &\frac{1}{r}\frac{\partial(r\tau_{xr})}{\partial r} + \frac{\partial \sigma_x}{\partial x} = \rho \frac{\partial^2 u_x}{\partial t^2} \end{aligned} \tag{2}$$

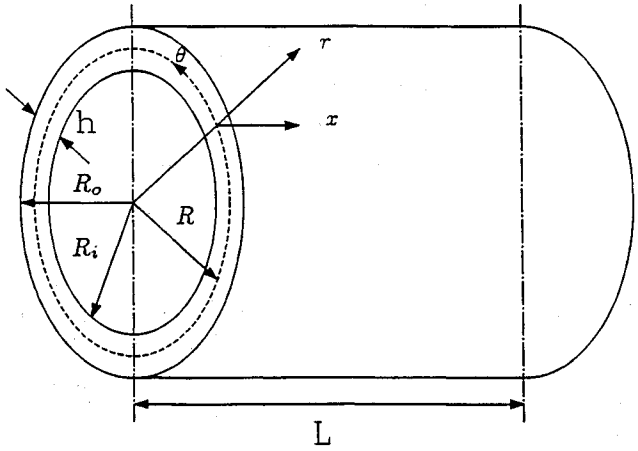

Fig. 1 Coordinates system and geometry of cylindrical shells.

where u_r, u_θ, and u_x denote the displacements in the radial, circumferential, and axial directions, respectively, with ρ denoting the mass density.

The strain-displacement relations of the cylindrical coordinate system are expressed as follows:

$$\begin{aligned} &\epsilon_x = \frac{\partial u_x}{\partial x}; \qquad && \epsilon_\theta = \frac{u_r}{r} \\ &\epsilon_r = \frac{\partial u_r}{\partial r}; \qquad && \gamma_{r\theta} = \frac{-u_\theta}{r} + \frac{\partial u_\theta}{\partial r} \\ &\gamma_{xr} = \frac{\partial u_x}{\partial r} + \frac{\partial u_r}{\partial x}; \qquad && \gamma_{x\theta} = \frac{\partial u_\theta}{\partial x} \end{aligned} \tag{3}$$

Substituting Eqs. (1) and (3) into Eq. (2), the governing equations in terms of displacements for each layer become

$$\begin{aligned} &C_{33}\frac{\partial^2 u_r}{\partial r^2} + C_{33}\frac{\partial u_r}{r\partial r} + C_{55}\frac{\partial^2 u_r}{\partial x^2} - C_{22}\frac{u_r}{r^2} \\ &\quad + (C_{36} - C_{45} - C_{26})\frac{\partial u_\theta}{r\partial x} + (C_{36} + C_{45})\frac{\partial^2 u_\theta}{\partial x \partial r} \\ &\quad + (C_{13} - C_{12})\frac{\partial u_x}{r\partial x} + (C_{13} + C_{55})\frac{\partial^2 u_x}{\partial x \partial r} = \rho \frac{\partial^2 u_r}{\partial t^2} \end{aligned} \tag{4a}$$

$$\begin{aligned} &(2C_{45} + C_{26})\frac{\partial u_r}{r\partial x} + (C_{45} + C_{36})\frac{\partial^2 u_r}{\partial r \partial x} + C_{44}\frac{\partial^2 u_\theta}{\partial r^2} \\ &\quad + C_{44}\frac{\partial u_\theta}{r\partial r} - C_{44}\frac{u_\theta}{r^2} + C_{66}\frac{\partial^2 u_\theta}{\partial x^2} + C_{45}\frac{\partial^2 u_x}{\partial r^2} \\ &\quad + 2C_{45}\frac{\partial u_x}{r\partial r} + C_{16}\frac{\partial^2 u_x}{\partial x^2} = \rho \frac{\partial^2 u_\theta}{\partial t^2} \end{aligned} \tag{4b}$$

$$\begin{aligned} &(C_{12} + C_{55})\frac{\partial u_r}{r\partial x} + (C_{13} + C_{55})\frac{\partial^2 u_r}{\partial r \partial x} + C_{45}\frac{\partial^2 u_\theta}{\partial r^2} + C_{16}\frac{\partial^2 u_\theta}{\partial x^2} \\ &\quad + C_{11}\frac{\partial^2 u_x}{\partial x^2} + C_{55}\frac{\partial^2 u_x}{\partial r^2} + C_{55}\frac{\partial u_x}{r\partial r} = \rho \frac{\partial^2 u_x}{\partial t^2} \end{aligned} \tag{4c}$$

It should be noted that the three PDEs are coupled together for arbitrarily laminated anisotropic cylinders, whereas the equation governing the circumferential displacement u_θ is uncoupled from the other two for cross-ply laminates. Moreover, the governing equations, Eqs. (4), are differential equations with variable coefficients and are not easily solved using a power series method. Therefore, an approximation is made for simplifying these governing equations. Introducing the radial local coordinate ξ_k located at the center of the kth artificial layer, and making the approximation $\xi_k/R_k \ll 1$, in which each layer is viewed as a thin coaxial cylinder, the following equations are assumed[15,18]:

$$\frac{1}{r} = \frac{1}{R_k}(1 - \eta_k); \qquad \frac{1}{r^2} = \frac{1}{R_k^2}(1 - 2\eta_k) \tag{5}$$

where

$$\xi_k = r - R_k; \qquad \eta_k = \xi_k / R_k$$

and k ranges from 1 to M, where M represents the total number of fictitious sublayers. Upon inserting Eq. (5) into Eqs. (4) and retaining the zeroth-order term, one obtains

$$\begin{aligned} &C_{33}^k\frac{\partial^2 u_r^k}{\partial \eta_k^2} + C_{33}^k\frac{\partial u_r^k}{\partial \eta_k} + C_{55}^k R_k^2\frac{\partial^2 u_r^k}{\partial x^2} - C_{22}^k u_r^k \\ &\quad + R_k\left[(C_{36}^k - C_{45}^k - C_{26}^k)\frac{\partial u_\theta^k}{\partial x} + (C_{36}^k + C_{45}^k)\frac{\partial^2 u_\theta^k}{\partial x \partial \eta_k}\right. \\ &\quad \left. + (C_{13}^k - C_{12}^k)\frac{\partial u_x^k}{\partial x} + (C_{13}^k + C_{55}^k)\frac{\partial^2 u_x^k}{\partial x \partial \eta_k}\right] = \rho^k R_k^2\frac{\partial^2 u_r^k}{\partial t^2} \end{aligned} \tag{6a}$$

$$R_k\left[(2C_{45}^k + C_{26}^k)\frac{\partial u_r^k}{\partial x} + (C_{45}^k + C_{36}^k)\frac{\partial^2 u_r^k}{\partial \eta_k \partial x}\right] + C_{44}^k \frac{\partial^2 u_\theta^k}{\partial \eta_k^2} + C_{44}^k \frac{\partial u_\theta^k}{\partial \eta_k} - C_{44}^k u_\theta^k + R_k^2 C_{66}^k \frac{\partial^2 u_\theta^k}{\partial x^2} + C_{45}^k \frac{\partial^2 u_x^k}{\partial \eta_k^2} + 2C_{45}^k \frac{\partial u_x^k}{\partial \eta_k} + R_k^2 C_{16}^k \frac{\partial^2 u_x^k}{\partial x^2} = \rho^k R_k^2 \frac{\partial^2 u_\theta^k}{\partial t^2} \tag{6b}$$

$$R_k\left[(C_{12}^k + C_{55}^k)\frac{\partial u_r^k}{\partial x} + (C_{13}^k + C_{55}^k)\frac{\partial^2 u_r^k}{\partial \eta_k \partial x}\right] + C_{45}^k \frac{\partial^2 u_\theta^k}{\partial \eta_k^2} + R_k^2 C_{16}^k \frac{\partial^2 u_\theta^k}{\partial x^2} + R_k^2 C_{11}^k \frac{\partial^2 u_x^k}{\partial x^2} + C_{55}^k \frac{\partial^2 u_x^k}{\partial \eta_k^2} + C_{55}^k \frac{\partial u_x^k}{\partial \eta_k} = \rho^k R_k^2 \frac{\partial^2 u_x^k}{\partial t^2} \tag{6c}$$

The resulting governing equations (6) become a set of differential equations with constant coefficients for which the solution is easier to obtain.

Solution of Governing Equation

For the static problem, the Navier-Stokes series solution for each layer takes the form

$$u_r^k = \sum_{m=1}^{\infty} A_r^k(\eta_k)\sin(p_m x)$$

$$u_\theta^k = \sum_{m=1}^{\infty} A_\theta^k(\eta_k)\cos(p_m x) \tag{7}$$

$$u_x^k = \sum_{m=1}^{\infty} A_x^k(\eta_k)\cos(p_m x)$$

where $p_m = m\pi/L$. The choice of this displacement field will automatically satisfy the following simply supported boundary condition at two ends of the cylinder, i.e.,

$$u_r = \sigma_x = \tau_{x\theta} = 0 \qquad \text{at} \qquad x = 0, L \tag{8}$$

Using Eqs. (6) and (7) yields

$$C_{33}^k \frac{d^2 A_r^k}{d\eta_k^2} + C_{33}^k \frac{dA_r^k}{d\eta_k} - p_m^2 R_k^2 C_{55}^k A_r^k - C_{22}^k A_r^k - p_m R_k\left[(C_{36}^k - C_{45}^k - C_{26}^k)A_\theta^k + (C_{36}^k + C_{45}^k)\frac{dA_\theta^k}{d\eta_k} + (C_{13}^k - C_{12}^k)A_x^k + (C_{13}^k + C_{55}^k)\frac{dA_x^k}{d\eta_k}\right] = 0 \tag{9a}$$

$$p_m R_k\left[(2C_{45}^k + C_{26}^k)A_r^k + (C_{45}^k + C_{36}^k)\frac{dA_r^k}{d\eta_k}\right] + C_{44}^k \frac{d^2 A_\theta^k}{d\eta_k^2} + C_{44}^k \frac{dA_\theta^k}{d\eta_k} - C_{44}^k A_\theta^k - p_m^2 R_k^2 C_{66}^k A_\theta^k + C_{45}^k \frac{d^2 A_x^k}{d\eta_k^2} + 2C_{45}^k \frac{dA_x^k}{d\eta_k} - p_m^2 R_k^2 C_{16}^k A_x^k = 0 \tag{9b}$$

$$p_m R_k\left[(C_{12}^k + C_{55}^k)A_r^k + (C_{13}^k + C_{55}^k)\frac{dA_r^k}{d\eta_k}\right] + C_{45}^k \frac{d^2 A_\theta^k}{d\eta_k^2} - p_m^2 R_k^2 C_{16}^k A_\theta^k - p_m^2 R_k^2 C_{11}^k A_x^k + C_{55}^k \frac{d^2 A_x^k}{d\eta_k^2} + C_{55}^k \frac{dA_x^k}{d\eta_k} = 0 \tag{9c}$$

where d denotes a derivative.

Equations (9a–9c) are three coupled ODEs with constant coefficients. The homogeneous solution may be obtained by assuming A_r^k, A_θ^k, and A_x^k in the form of $e^{\lambda_{mn}^k \eta_k}$ $(n = 1 \sim 6)$, and the corresponding characteristic equation is

$$a_6(\lambda_{mn}^k)^6 + a_5(\lambda_{mn}^k)^5 + a_4(\lambda_{mn}^k)^4 + a_3(\lambda_{mn}^k)^3 + a_2(\lambda_{mn}^k)^2 + a_1\lambda_{mn}^k + a_0 = 0 \tag{10}$$

where $a_i (i = 0 \sim 6)$ are listed in Eq. (A1). When the six distinct real roots are obtained, general solutions of displacements and stresses can be given as follows:

$$u_r^k = \sum_{m=1}^{\infty}\sum_{n=1}^{6} A_{mn}^k e^{\lambda_{mn}^k \eta_k}\sin(p_m x)$$

$$u_\theta^k = \sum_{m=1}^{\infty}\sum_{n=1}^{6} A_{mn}^k \phi_{mn}^k e^{\lambda_{mn}^k \eta_k}\cos(p_m x)$$

$$u_x^k = \sum_{m=1}^{\infty}\sum_{n=1}^{6} A_{mn}^k \Omega_{mn}^k e^{\lambda_{mn}^k \eta_k}\cos(p_m x)$$

$$\sigma_r^k = \sum_{m=1}^{\infty}\sum_{n=1}^{6}\left[-p_m C_{13}^k \Omega_{mn}^k + \frac{C_{23}^k}{r} + C_{33}^k \frac{\lambda_{mn}^k}{R_k} - p_m C_{36}^k \phi_{mn}^k\right] e^{\lambda_{mn}^k \eta_k} A_{mn}^k \sin(p_m x)$$

$$\sigma_\theta^k = \sum_{m=1}^{\infty}\sum_{n=1}^{6}\left[-p_m C_{12}^k \Omega_{mn}^k + \frac{C_{22}^k}{r} + C_{23}^k \frac{\lambda_{mn}^k}{R_k} - p_m C_{26}^k \phi_{mn}^k\right] e^{\lambda_{mn}^k \eta_k} A_{mn}^k \sin(p_m x)$$

$$\sigma_x^k = \sum_{m=1}^{\infty}\sum_{n=1}^{6}\left[-p_m C_{11}^k \Omega_{mn}^k + \frac{C_{12}^k}{r} + C_{13}^k \frac{\lambda_{mn}^k}{R_k} - p_m C_{16}^k \phi_{mn}^k\right] e^{\lambda_{mn}^k \eta_k} A_{mn}^k \sin(p_m x) \tag{11}$$

$$\tau_{r\theta}^k = \sum_{m=1}^{\infty}\sum_{n=1}^{6}\left[C_{44}^k\left(\frac{-\phi_{mn}^k}{r} + \frac{\lambda_{mn}^k}{R_k}\phi_{mn}^k\right) + C_{45}^k\left(\frac{\lambda_{mn}^k}{R_k}\Omega_{mn}^k + p_m\right)\right] e^{\lambda_{mn}^k \eta_k} A_{mn}^k \cos(p_m x)$$

$$\tau_{xr}^k = \sum_{m=1}^{\infty}\sum_{n=1}^{6}\left[C_{45}^k\left(\frac{-\phi_{mn}^k}{r} + \frac{\lambda_{mn}^k}{R_k}\phi_{mn}^k\right) + C_{55}^k\left(\frac{\lambda_{mn}^k}{R_k}\Omega_{mn}^k + p_m\right)\right] e^{\lambda_{mn}^k \eta_k} A_{mn}^k \cos(p_m x)$$

$$\tau_{x\theta}^k = \sum_{m=1}^{\infty}\sum_{n=1}^{6}\left[-p_m C_{16}^k \Omega_{mn}^k + \frac{C_{26}^k}{r} + C_{36}^k \frac{\lambda_{mn}^k}{R_k} - p_m C_{66}^k \phi_{mn}^k\right] e^{\lambda_{mn}^k \eta_k} A_{mn}^k \sin(p_m x)$$

where the constants ϕ_{mn}^k and Ω_{mn}^k are expressed in Eq. (A2). If complex roots exist, the solution is expressed in Eq. (A3). Equations (A1–A3) are listed in the Appendix. It should be noted that Eqs. (11) contain $6M$ undetermined coefficients for any fixed m value. These constants can be obtained by using the traction conditions on the inner and outer surfaces, usually expanded into Fourier series, and the continuity conditions of

displacements and transverse stresses at the interfaces (both real and fictitious), which are stated as follows:

$$\sigma_r = q_i; \quad q_i = \sum_{m=1}^{\infty} q_{im}\sin(p_m x) \quad \text{at} \quad \eta_k = h_M/2R_M$$

$$\sigma_r = q_o; \quad q_o = \sum_{m=1}^{\infty} q_{om}\sin(p_m x) \quad \text{at} \quad \eta_k = h_1/2R_1$$

$$\begin{aligned}
&\tau_{r\theta} = \tau_{xr} = 0 \quad \text{at} \quad \eta_k = h_1/2R_1,\ h_M/2R_M \\
&u_r^k(x, -h_k/2R_k) = u_r^{k+1}(x, h_{k+1}/2R_{k+1}) \\
&u_\theta^k(x, -h_k/2R_k) = u_\theta^{k+1}(x, h_{k+1}/2R_{k+1}) \\
&u_x^k(x, -h_k/2R_k) = u_x^{k+1}(x, h_{k+1}/2R_{k+1}) \\
&\sigma_r^k(x, -h_k/2R_k) = \sigma_r^{k+1}(x, h_{k+1}/2R_{k+1}) \\
&\tau_{r\theta}^k(x, -h_k/2R_k) = \tau_{r\theta}^{k+1}(x, h_{k+1}/2R_{k+1}) \\
&\tau_{xr}^k(x, -h_k/2R_k) = \tau_{xr}^{k+1}(x, h_{k+1}/2R_{k+1})
\end{aligned} \tag{12}$$

After solving the $6M$ unknown constants, and substituting them into Eqs. (11), the resulting displacements and stresses can be obtained.

Numerical Results and Discussion

A numerical convergence study is necessary because of the approximate nature of the procedures. The problem considered here is for a single anisotropic layer [45 deg] subjected to sinusoidal normal loading on the outer surface $q_o = p_0\sin(\pi x/L)$. Material properties and nondimensionalized deformations and stresses are considered as follows:

$$\begin{aligned}
&E_L/E_T = 40; \quad G_{LT}/E_T = 0.5; \quad G_{TT}/E_T = 0.2 \\
&\nu_{LT} = 0.25; \quad \nu_{TT} = 0.49; \quad S = \frac{R}{h}; \quad \frac{L}{R} = 20 \\
&(\bar{u}_r, \bar{u}_\theta, \bar{u}_x) = \frac{E_T h}{p_0 R^2}(10u_r, 20u_\theta, u_x) \\
&(\bar{\sigma}_r, \bar{\sigma}_\theta, \bar{\sigma}_x, \bar{\tau}_{r\theta}, \bar{\tau}_{xr}, \bar{\tau}_{x\theta}) = \frac{1}{p_0}(\sigma_r, \sigma_\theta, \sigma_x, \tau_{r\theta}, \tau_{xr}, \tau_{x\theta})
\end{aligned} \tag{13}$$

Table 1 Convergence study for 45-deg layer with $S = 20$

M	$\bar{u}_r$ $(L/2, R)$	$\bar{\sigma}_x$ $(L/2, R_o)$	$\bar{\sigma}_\theta$ $(L/2, R_o)$	$\bar{\tau}_{x\theta}$ $(L/2, R_o)$	$\bar{\tau}_{r\theta}$ (L, R)	$\bar{\tau}_{xr}$ (L, R)
1	7.6356	−6.7511	13.2727	6.9453	−0.01358	−0.00600
2	7.6162	−6.7489	13.2230	6.9375	−0.01410	−0.01355
5	7.6109	−6.7483	13.2091	6.9381	−0.01407	−0.01324
10	7.6101	−6.7482	13.2071	6.9382	−0.01409	−0.01354
15	7.6100	−6.7482	13.2067	6.9382	−0.01409	−0.01351
20	7.6099	−6.7482	13.2066	6.9382	−0.01409	−0.01354

Table 2 Convergence study for 45-deg layer with $S = 5$

M	$\bar{u}_r$ $(L/2, R)$	$\bar{\sigma}_x$ $(L/2, R_o)$	$\bar{\sigma}_\theta$ $(L/2, R_o)$	$\bar{\tau}_{x\theta}$ $(L/2, R_o)$	$\bar{\tau}_{r\theta}$ (L, R)	$\bar{\tau}_{xr}$ (L, R)
1	7.7507	−5.5944	−0.4584	5.5408	−0.04420	−0.01757
2	7.4495	−5.3541	−0.3785	5.3102	−0.03197	−0.02610
5	7.4083	−5.2897	−0.3573	5.2477	−0.04653	−0.04384
10	7.3979	−5.2805	−0.3543	5.2388	−0.04667	−0.04493
15	7.3960	−5.2789	−0.3537	5.2372	−0.04663	−0.04478
20	7.3953	−5.2783	−0.3535	5.2366	−0.04664	−0.04490

Two mean-radius-to-thickness ratios S are used, and the corresponding solutions are listed in Tables 1 and 2, respectively. The number of fictitious layers M ranges from 1 to 20. The radial displacement and five stresses listed in these tables suggest that the convergence is very fast even for a thick cylinder. Therefore, the ratio $h_k/R_k \le 1/100$ is used in the following numerical analysis: for two-layer laminates, h_k/R_k is 1/100; for three-layer laminates, 1/105.

The results of deformations and stresses of a two-layer unsymmetric laminate [−45/0 deg] and a symmetric angle-ply laminate [−45/45/−45 deg] closed cylinder under sinusoidal normal loading are listed in Tables 3 and 4, respectively, together with results from classical shell theory (CST). The negative sign of the fiber angle denotes counterclockwise direction with respect to the positive direction of the generator (x axis). The layers are of equal thickness. In these tables, the ratio S ranges from 5 to 500. It may be seen that for higher ratios of S the present approximate elasticity solution approaches the CST result.

In the second example, the same laminates [−45/0 deg] and [−45/45/−45 deg], subjected to a uniform internal pressure, are analyzed with the same material properties and boundary condition. The S used here is only 5. Figure 2 gives the radial deflections at $r = R$ along the cylinder axis from the present and CST solutions for both stacking sequences. It should be noted that the initial pressure is applied on the inner surface instead of the middle surface, as in CST. In the central region, the deflections are all very uniform. Some variations can be seen in the edge region, just as in the case of isotropic shells. Figures 3–5 show the axial variation of in-plane stresses of the outer and inner surfaces for the [−45/0 deg] lamination. From these figures, it is found that the stresses σ_x, σ_θ, and $\tau_{x\theta}$ at the inner surface in the central region are very close for both theories. The stresses σ_θ and $\tau_{x\theta}$ are almost identical in the present and CST solution for the edge region; this is not the case with stress σ_x. Furthermore, the CST results on the stresses σ_x, σ_θ, and $\tau_{x\theta}$ at the outer surface of the outer layer have the same tendency in the CST as in the present solution, but the values disagree considerably.

Axial variations of in-plane stresses for the [−45/45/−45 deg] lamination are shown in Figs. 6–8. These figures show the stresses at the outer surface of the outer layer and the inner

Table 3 Comparisons of displacement and stresses between present and CST solution for [45/0 deg] lamination under sinusoidal normal loading of the outer surface

R/h	Theory	$\bar{u}_r(L/2, R)$	$\bar{\sigma}_x(L/2, R_o)$	$\bar{\sigma}_\theta(L/2, R_o)$	$\bar{\tau}_{x\theta}(L/2, R_o)$	$\bar{\tau}_{r\theta}(L, R)$	$\bar{\tau}_{xr}(L, R)$
5	Present	7.5471	−0.2043	3.2292	−2.2507	−0.02042	−0.05179
	CST	7.1654	−0.0768	3.5840	−1.7734	—	—
10	Present	7.2755	2.5192	9.5131	−1.0300	−0.02238	−0.04932
	CST	7.0587	2.8217	10.055	−0.3753	—	—
20	Present	7.1016	8.4264	22.526	1.9028	−0.02331	−0.04831
	CST	6.9868	8.8086	23.150	2.6390	—	—
50	Present	6.9849	26.482	61.875	11.062	−0.02384	−0.04778
	CST	6.9372	26.901	62.537	11.837	—	—
100	Present	6.9436	56.658	127.530	26.420	−0.02401	−0.04761
	CST	6.9196	57.097	128.212	27.215	—	—
500	Present	6.9100	298.270	652.960	149.509	−0.02414	−0.04748
	CST	6.9052	298.724	653.657	150.319	—	—

Table 4 Comparisons of displacement and stresses between present and CST solution for [−45/45/−45 deg] lamination under sinusoidal normal loading of the outer surface

R/h	Theory	$\bar{u}_r(L/2, R)$	$\bar{\sigma}_x(L/2, R_o)$	$\bar{\sigma}_\theta(L/2, R_o)$	$\bar{\tau}_{x\theta}(L/2, R_o)$	$\bar{\tau}_{r\theta}(L, R)$	$\bar{\tau}_{xr}(L, R)$
5	Present	5.6624	−2.4456	2.7546	−0.4057	0.01327	0.01738
	CST	5.2674	−0.6488	4.3447	1.6383	—	—
10	Present	5.4903	−3.3360	6.8694	1.0235	0.00720	0.00946
	CST	5.2675	−1.2117	8.7819	3.3755	—	—
20	Present	5.3861	−4.6095	15.602	4.3612	0.00370	0.00486
	CST	5.2675	−2.3313	17.662	6.8564	—	—
50	Present	5.3168	−8.0515	42.165	14.728	0.00173	0.00173
	CST	5.2675	−5.6859	44.308	17.304	—	—
100	Present	5.2924	−13.670	86.548	32.115	0.00087	0.00087
	CST	5.2675	−11.276	88.718	34.717	—	—
500	Present	5.2725	−58.408	441.810	171.402	0.00017	0.00017
	CST	5.2675	−55.992	444.001	174.025	—	—

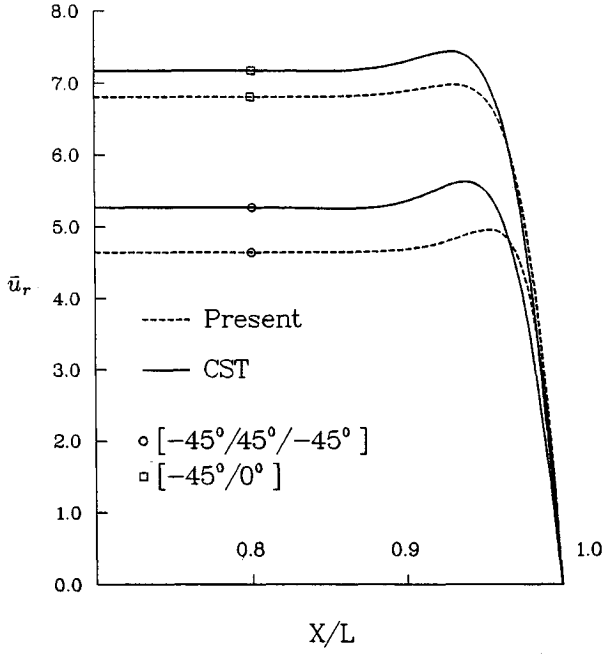

Fig. 2 Axial variation of radial deflection for the [−45/0 deg] and [−45/45/−45 deg] laminations.

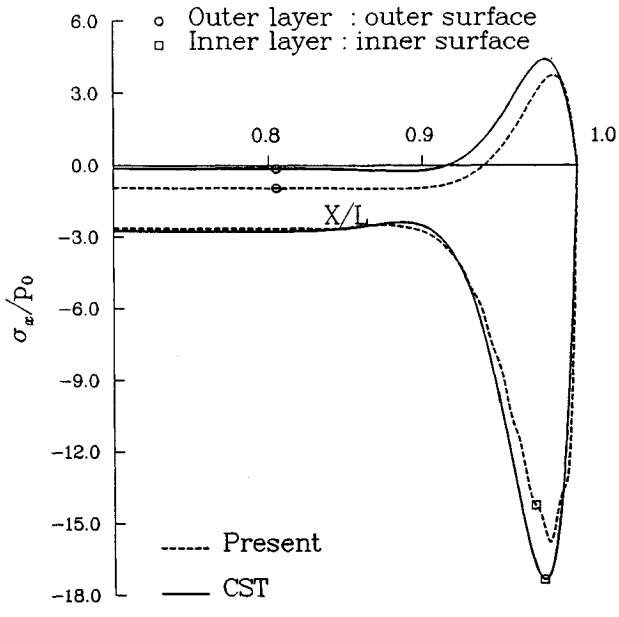

Fig. 3 Axial variation of longitudinal stresses on the outer and inner surfaces for the [−45/0 deg] lamination.

surface of the inner layer. The CST solution shows considerable disagreement when compared with the present solution. This tendency exists not only in the edge region but also in the central region. It has been suggested[21] that the reason for the difference is the change in shear angle from layer to layer and the insensitivity of the CST to this change. The results of the present study suggest that the change of shear angle may not be the reason, the transverse shear stress in the central region being almost zero, as can be seen from Fig. 9. Actually, the initial curvature effect, combined with the material properties, accounts for the difference. In this analysis the initial curvature effect means using a different radius of curvature for each different fictitious layer instead of a single radius of curvature for the whole shell as in CST. Hence, as the laminate becomes thicker, the difference between the radii of curvature of the inner and outer surfaces increases. In another sense, this effect can be explained in terms of thickness. In calculating σ_x, and also σ_θ and $\tau_{x\theta}$, the hoop strain ϵ_θ is involved as well as the radius of curvature. The radius of curvature is smaller on the inner surface than the mean radius, and larger on the outer surface. The difference is not negligible, being almost 20% in the case studied here. Furthermore, as shown by the constitutive equation under this stacking sequence, the corresponding material constant, e.g., C_{12} for σ_x, is comparable to the major constant, e.g., C_{11}; the influence of ϵ_θ on σ_x, σ_θ, and $\tau_{x\theta}$ is then obvious. Consequently, the results from CST on both surfaces are very close, falling between the results for the outer and inner surfaces in the present approach, as can be seen in Figs. 6-8. The two curves are separated by the initial curvature effect; that is, the one on the outer surface is lowered by its larger curvature, whereas the one on the inner surface is raised by its smaller curvature. The influence of the initial curvature effect can also be observed from the results of stresses at interfaces (not shown).

It should be noted that, in Fig. 6, results from finite element analysis are also given for comparison. Although the solution of the present approximation does converge, as can be seen from the convergence study, it is not necessary to be exact. To doublecheck the accuracy of the present analysis, the results from a three-dimensional, layerwise finite element analysis[22] are shown in Fig. 6. In this figure, it is found that the agreement between the present analysis and finite element is acceptable.

As for the transverse shear stress τ_{xr}, Fig. 9 shows the variations at the outer interface, the middle surface, and the inner interface along the axial direction. It can be observed that τ_{xr} is zero in the central region, reaching higher values at the edge; the middle surfaces show maximum transverse shear stress at the endpoints. The axial variations of in-plane displacements u_x and u_θ, as shown in Fig. 10, give a clear view of how the shell deforms. In the central region, the strains are quite uniform. For axial displacement u_x, the difference be-

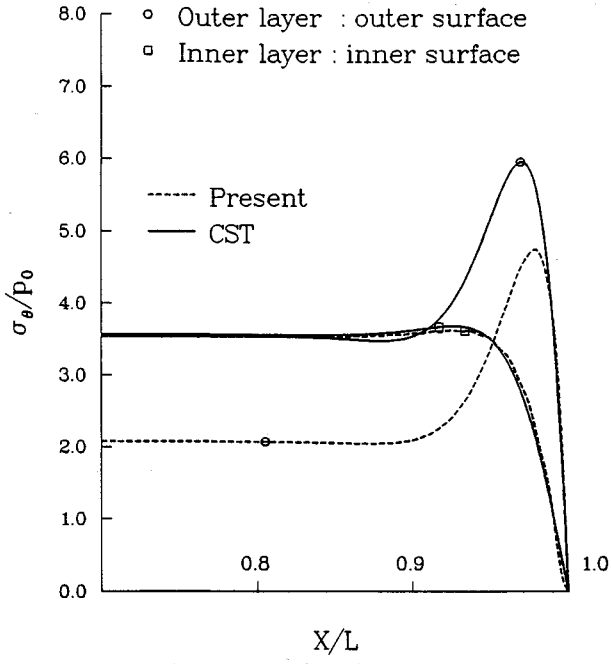

Fig. 4 Axial variation of circumferential stresses on the outer and inner surfaces for the [−45/0 deg] lamination.

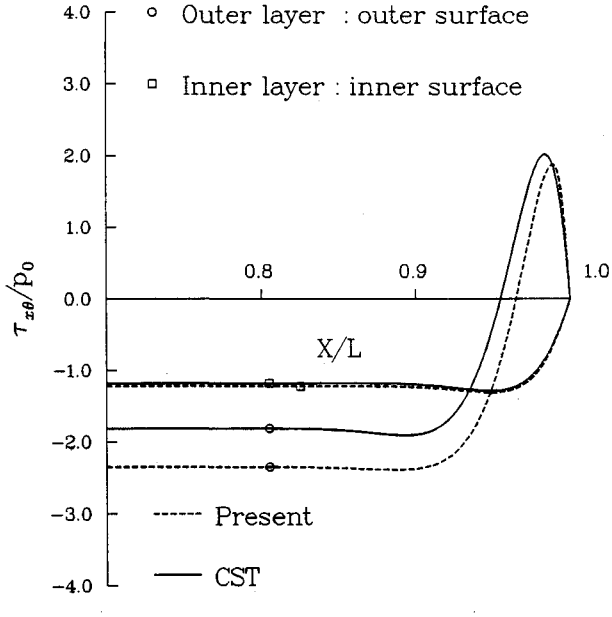

Fig. 5 Axial variation of in-plane shear stresses on the outer and inner surfaces for the [−45/0 deg] lamination.

tween the outer and inner surfaces is not very pronounced even in the edge region. On the other hand, the through-the-thickness variation of the u_θ in the central region is noticeable, clearly showing the effect of coupling.

In all of the figures, the boundary-layer phenomenon is obvious. In the literature surveyed, the boundary-layer size is characterized by the following two methods. In the first method, a criterion proposed by Vinson and Chou[23] for a single anisotropic layer is used for generally laminated, anisotropic closed cylinders, under the restricted conditions of long shell behavior. Only the one-sided (right-hand side) boundary layer is discussed because of symmetry. This region is located at $e^{-\beta(L-x_b)} \geq 0.006$ (see Ref. 23; for β, see Ref. 20). After calculation, the region locates at $0.8728 \leq x_b/L \leq 1.0$ for [−45/0 deg] and $0.8653 \leq x_b/L \leq 1.0$ for [−45/45/−45 deg]. It should be noted that this criterion is based on CST and cannot be used in thick shells; these values are for reference only. In the second method, Pagano and Whitney[24] proposed a conservative estimate for the size of the boundary-layer region, i.e., $(L-2R)/L \leq x_b/L \leq 1.0$. Applied to this problem it is $0.9 \leq x/L \leq 1.0$. Because there is no such criterion as the one proposed by Vinson and Chou[23] within the framework of elasticity theory, a criterion based on an engineering judgment of the variation of deflection starting above 5%, compared with the maximum deflection, is proposed here, i.e.,

$$\frac{u_{r_x} - u_{r_c}}{u_{r_{\max}} - u_{r_c}} = 0.05 \tag{14}$$

In the previous formula, $u_{r_{\max}}$ and u_{r_c} denote maximum and central radial displacements along the generator, whereas u_{r_x} is the deflection corresponding to the starting point of the boundary layer. According to this criterion, the boundary-layer region calculated from the present results is $0.8620 \leq$

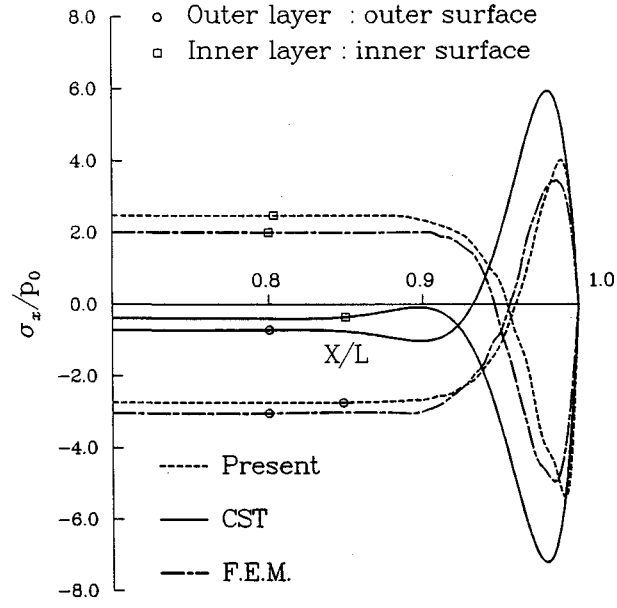

Fig. 6 Axial variation of longitudinal stresses on the outer and inner surfaces for the [−45/45/−45 deg] lamination.

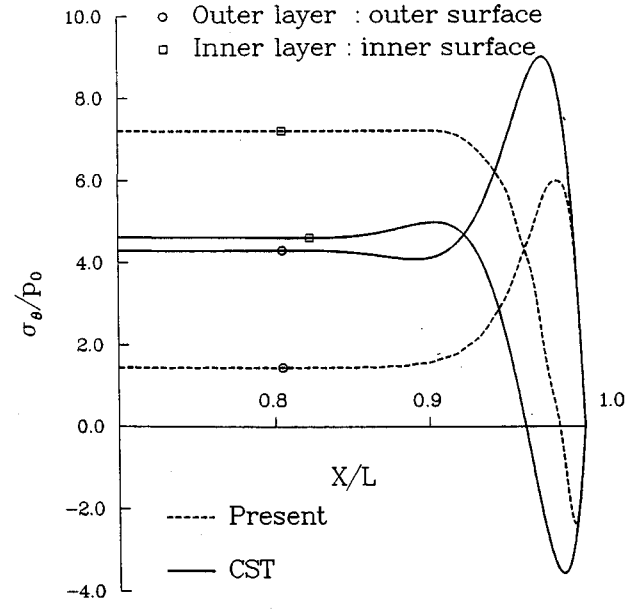

Fig. 7 Axial variation of circumferential stresses on the outer and inner surfaces for the [−45/45/−45 deg] lamination.

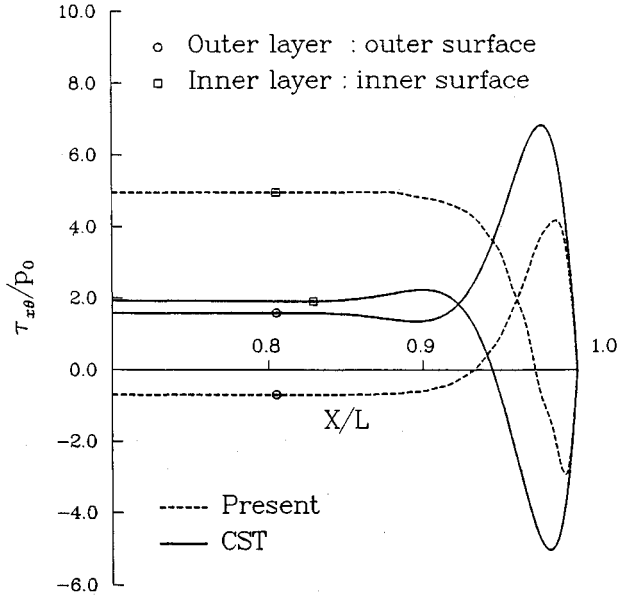

Fig. 8 Axial variation of in-plane shear stresses on the outer and inner surfaces for the [−45/45/−45 deg] lamination.

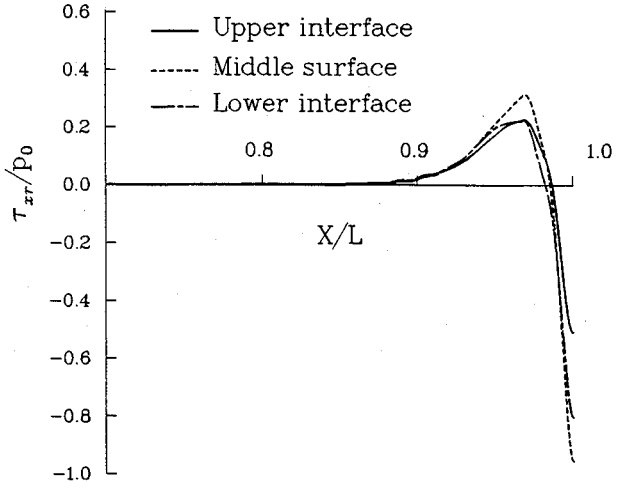

Fig. 9 Axial variation of transverse shear stresses τ_{xr} on the upper interface, middle surface, and lower interface for the [−45/45/−45 deg] lamination.

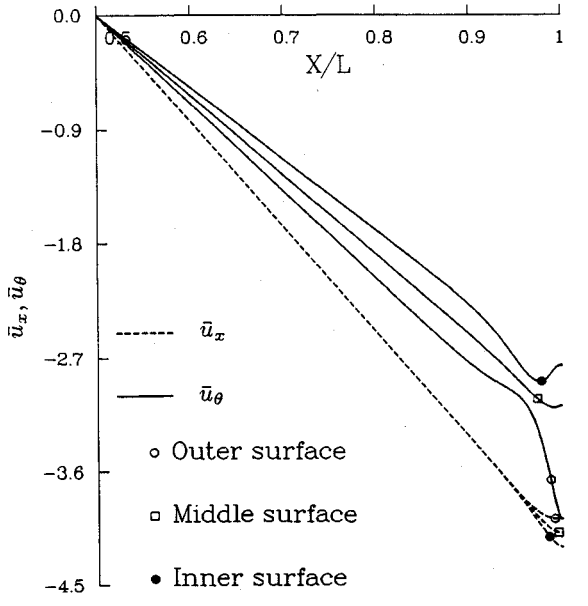

Fig. 10 Axial variation of longitudinal and circumferential displacements on the outer surface, middle surface, and inner surface for the [−45/45/−45 deg] lamination.

$x_b/L \leq 1.0$ for [−45/0 deg] and $0.8800 \leq x_b/L \leq 1.0$ for [−45/45/−45 deg]. No matter which theory or criterion is used, the region proposed by Pagano and Whitney[24] seems to be not conservative enough for the problem considered here, suggesting that a more conservative value $(L-3R)/L \leq x_b/L \leq 1.0$, i.e., $0.85 \leq x_b/L \leq 1.0$ may be appropriate. However, before drawing a conclusion, intensive study of the boundary layer of arbitrarily laminated, anisotropic thick closed cylinders is needed. Such a solution would be a function of lamination, geometry, anisotropy, loading, and end conditions.

Conclusions

An approximate elasticity solution for arbitrarily laminated, anisotropic cylindrical closed shells of finite length with simply supported end conditions is presented in this paper. The highly coupled PDEs can be reduced to ODEs of variable coefficients by choosing a solution composed of trigonometric functions along the axial direction. This can be further reduced to ODEs with constant coefficients. From the preliminary results shown in this study, it is found that the general behavior of laminated shells is similar to that of isotropic shells, uniform deflection in the central region, and a clear boundary layer. Although the deflection is uniform in the central position, the in-plane stresses are not constant through the thickness as in the case of isotropic shells. The coupling effects, such as bending stretching and stretching twisting, are thought to be responsible. The transverse shear stresses are zero in the central region but not negligible at the edge for the case studied here. The initial curvature effect is very important in making accurate predictions of stresses even in the central region. Consequently, this study shows that if a good two-dimensional shell theory is to be established, with satisfactory accuracy for both deformations and stresses, shear effect and initial curvature effect must be included. As for boundary layer, a conservative value $(L-3R)/L \leq x_b/L \leq 1.0$ would seem to be appropriate for the influence region.

Appendix

The constants $a_i (i = 0 \sim 6)$ in Eq. (10) are

$$a_6 = b_1 - b_{22}; \qquad a_5 = 3a_6$$

$$a_4 = 2b_1 - C_{44}^k(b_3 + C_{55}^k b_2) - b_4 - 2C_{45}^k b_8 + C_{55}^k b_{18} - 2b_{22} + 2b_{23} + b_2 b_{24} + C_{44}^k b_{28}$$

$$a_3 = -b_1 - 2C_{44}^k(b_3 + C_{55}^k b_2) - 2b_4 - C_{45}^k(2b_8 + b_9 + b_{14}) + 2C_{55}^k b_{18} + 4b_{23} + 2b_2 b_{24} + 2C_{44}^k b_{28}$$

$$a_2 = -b_1 + b_2(b_5 - 2b_{25}) - b_4 + b_6(b_3 + C_{55}^k b_2) - C_{45}^k(2b_9 + b_{10} + b_{15}) + 2C_{16}^k b_{11} + C_{55}^k(b_{18} + b_{19}) - C_{11}^k b_{20} + 2b_{23} - b_{26} + C_{44}^k b_{29} - C_{66}^k b_{30} \qquad \text{(A1)}$$

$$a_1 = (C_{44}^k + b_6)(b_3 + C_{55}^k b_2) + b_2(b_5 - 2b_{25}) - 2C_{45}^k b_{10} + C_{16}^k(b_{12} + b_{16}) + C_{55}^k b_{19} - C_{11}^k b_{20} - b_{26} + C_{44}^k(b_{29} - b_{28}) - C_{66}^k b_{30}$$

$$a_0 = b_2(b_{27} - b_5 - b_7) + C_{16}^k(b_{13} + b_{17}) - C_{11}^k b_{21} - C_{44}^k b_{29} - C_{66}^k b_{31}$$

where

$$b_1 = C_{33}^k C_{44}^k C_{55}^k; \quad b_2 = p_m^2 R_k^2 C_{55}^k + C_{22}^k; \quad b_3 = p_m^2 R_k^2 C_{11}^k C_{33}^k$$

$$b_4 = p_m^2 R_k^2 C_{33}^k C_{55}^k C_{66}^k; \qquad b_5 = p_m^2 R_k^2 C_{11}^k C_{44}^k; \quad b_6 = p_m^2 R_k^2 C_{66}^k$$

$$b_7 = p_m^4 R_k^4 C_{11}^k C_{66}^k; \qquad b_8 = p_m^2 R_k^2 (C_{36}^k + C_{45}^k)(C_{13}^k + C_{55}^k)$$

$$b_9 = p_m^2 R_k^2 [(C_{36}^k - C_{45}^k - C_{26}^k)(C_{13}^k + C_{55}^k) + (C_{36}^k + C_{45}^k)(C_{12}^k + C_{55}^k)]$$

$$b_{10} = p_m^2 R_k^2 (C_{36}^k - C_{45}^k - C_{26}^k)(C_{12}^k + C_{55}^k); \quad b_{11} = p_m^2 R_k^2 b_8$$

$$b_{12} = p_m^2 R_k^2 b_9; \qquad b_{13} = p_m^2 R_k^2 b_{10}$$

$$b_{14} = p_m^2 R_k^2 [(2C_{45}^k + C_{26}^k)(C_{13}^k + C_{55}^k) + (C_{13}^k - C_{12}^k)(C_{36}^k + C_{45}^k)]$$

$$b_{15} = p_m^2 R_k^2 (C_{13}^k - C_{12}^k)(2C_{45}^k + C_{26}^k); \qquad b_{16} = p_m^2 R_k^2 b_{14}$$

$$b_{17} = p_m^2 R_k^2 b_{15}; \qquad b_{18} = p_m^2 R_k^2 (C_{36}^k + C_{45}^k)^2$$

$$b_{19} = p_m^2 R_k^2 (C_{36}^k - C_{45}^k - C_{26}^k)(2C_{45}^k + C_{26}^k); \quad b_{20} = p_m^2 R_k^2 b_{18}$$

$$b_{21} = p_m^2 R_k^2 b_{19}; \qquad b_{22} = C_{33}^k C_{45}^{k^2}$$

$$b_{23} = p_m^2 R_k^2 C_{16}^k C_{33}^k C_{45}^k; \qquad b_{24} = C_{45}^{k^2}; \qquad b_{25} = p_m^2 R_k^2 C_{16}^k C_{45}^k$$

$$b_{26} = p_m^4 R_k^4 C_{16}^{k^2} C_{33}^k; \qquad b_{27} = p_m^4 R_k^4 C_{16}^{k^2}$$

$$b_{28} = p_m^2 R_k^2 (C_{13}^k + C_{55}^k)^2; \qquad b_{29} = p_m^2 R_k^2 (C_{13}^k - C_{12}^k)(C_{12}^k + C_{55}^k)$$

$$b_{30} = p_m^2 R_k^2 b_{28}; \qquad b_{31} = p_m^2 R_k^2 b_{29}$$

The constants ϕ_{mn}^k and Ω_{mn}^k in Eq. (11) are given as

$$\begin{aligned}\phi_{mn}^k = \frac{1}{\Delta_1} \{ & -p_m^2 R_k^2 [\lambda_{mn}^k (C_{13}^k + C_{55}^k) + C_{13}^k - C_{12}^k] \\ & \times [\lambda_{mn}^k (C_{36}^k + C_{45}^k) + 2C_{45}^k + C_{26}^k] \\ & - [C_{33}^k \lambda_{mn}^k (\lambda_{mn}^k + 1) - (p_m^2 R_k^2 C_{55}^k + C_{22}^k)] \\ & \times [C_{45}^k \lambda_{mn}^k (\lambda_{mn}^k + 2) - p_m^2 R_k^2 C_{16}^k]\}\end{aligned} \tag{A2}$$

$$\begin{aligned}\Omega_{mn}^k = \frac{1}{\Delta_1} \{ & [C_{33}^k \lambda_{mn}^k (\lambda_{mn}^k + 1) - (p_m^2 R_k^2 C_{55}^k + C_{22}^k)] \\ & \times [C_{44}^k \lambda_{mn}^k (\lambda_{mn}^k + 1) - (p_m^2 R_k^2 C_{66}^k + C_{44}^k)] \\ & + p_m^2 R_k^2 [\lambda_{mn}^k (C_{36}^k + C_{45}^k) + C_{36}^k - C_{45}^k - C_{26}^k] \\ & \times [\lambda_{mn}^k (C_{36}^k + C_{45}^k) + 2C_{45}^k + C_{26}^k]\}\end{aligned}$$

where

$$\begin{aligned}\Delta_1 = p_m R_k \{ & [\lambda_{mn}^k (C_{13}^k + C_{55}^k) + C_{13}^k - C_{12}^k] \\ & \times [C_{44}^k \lambda_{mn}^k (\lambda_{mn}^k + 1) - (p_m^2 R_k^2 C_{66}^k + C_{44}^k)] \\ & - [\lambda_{mn}^k (C_{36}^k + C_{45}^k) + C_{36}^k - C_{45}^k - C_{26}^k] \\ & \times [C_{45}^k \lambda_{mn}^k (\lambda_{mn}^k + 2) - p_m^2 R_k^2 C_{16}^k]\}\end{aligned}$$

For the complex roots obtained in Eq. (10), the solution of displacements and stresses are to be modified. In the following, two complex conjugated roots, $p_{m1} \pm iq_{m1}$, are assumed. For the sake of convenience, only displacement formulas are given as

$$\begin{aligned}u_r^k = & \sum_{m=1}^{\infty} \left\{ e^{p_{m1}} [A_{m1}^k \cos(q_{m1}\eta_k) + A_{m2}^k \sin(q_{m1}\eta_k)] \right. \\ & \left. + \sum_{n=3}^{6} e^{\lambda_{mn}^k \eta_k} A_{mn}^k \right\} \sin(p_m x) \\ u_\theta^k = & \sum_{m=1}^{\infty} \left\{ e^{p_{m1}} [f_{m1} \cos(q_{m1}\eta_k) + f_{m3} \sin(q_{m1}\eta_k)] A_{m1}^k \right. \\ & + e^{p_{m1}} [f_{m2} \cos(q_{m1}\eta_k) + f_{m4} \sin(q_{m1}\eta_k)] A_{m2}^k \\ & \left. + \sum_{n=3}^{6} \phi_{mn}^k e^{\lambda_{mn}^k \eta_k} A_{mn}^k \right\} \cos(p_m x) \\ u_x^k = & \sum_{m=1}^{\infty} \left\{ e^{p_{m1}} [f_{m5} \cos(q_{m1}\eta_k) + f_{m7} \sin(q_{m1}\eta_k)] A_{m1}^k \right. \\ & + e^{p_{m1}} [f_{m6} \cos(q_{m1}\eta_k) + f_{m8} \sin(q_{m1}\eta_k)] A_{m2}^k \\ & \left. + \sum_{n=3}^{6} \Omega_{mn}^k e^{\lambda_{mn}^k \eta_k} A_{mn}^k \right\} \cos(p_m x)\end{aligned} \tag{A3}$$

where

$$[f_{m1}, f_{m2}] = \frac{1}{\Delta_2} \{ [h_1, h_2](g_5 g_9 - g_6 g_8) + [h_3, h_4] \times (g_3 g_8 - g_2 g_9) + [h_5, h_6](g_2 g_6 - g_3 g_5) \}$$

$$[f_{m3}, f_{m4}] = \frac{1}{\Delta_2} \{ [h_1, h_2](g_6 g_7 - g_4 g_9) + [h_3, h_4] \times (g_1 g_9 - g_3 g_7) + [h_5, h_6](g_3 g_4 - g_1 g_6) \}$$

$$[f_{m5}, f_{m6}] = \frac{-e_1}{e_3} [f_{m1}, f_{m2}] + \frac{e_2}{e_3} [f_{m3}, f_{m4}] + \frac{e_4}{e_3} [f_{m7}, f_{m8}] + \left[\frac{d_1}{e_3}, \frac{-d_2}{e_3} \right]$$

$$[f_{m7}, f_{m8}] = \frac{1}{\Delta_2} \{ [h_1, h_2](g_4 g_8 - g_5 g_7) + [h_3, h_4] \times (g_2 g_7 - g_1 g_8) + [h_5, h_6](g_1 g_5 - g_2 g_4) \}$$

wherein

$$\Delta_2 = g_1 g_5 g_9 + g_2 g_6 g_7 + g_3 g_4 g_8 - g_2 g_4 g_9 - g_1 g_6 g_8 - g_3 g_5 g_7$$

$$g_1 = e_1 e_4 - e_2 e_3; \quad g_2 = -(e_2 e_4 + e_1 e_3); \quad g_3 = -(e_3^2 + e_4^2)$$

$$g_4 = e_1 e_7 - e_3 e_5; \quad g_5 = e_3 e_6 - e_2 e_7; \quad g_6 = e_3 e_8 - e_4 e_7$$

$$g_7 = e_1 e_8 - e_3 e_6; \quad g_8 = -(e_2 e_8 + e_3 e_5); \quad g_9 = -(e_4 e_8 + e_3 e_7)$$

$$h_1 = e_4 d_1 - e_3 d_2; \quad h_2 = -(e_4 d_2 + e_3 d_1); \quad h_3 = e_7 d_1 + e_3 d_3$$

$$h_4 = -(e_7 d_2 + e_3 d_4); \quad h_5 = e_8 d_1 + e_3 d_4$$

$$h_6 = e_3 d_3 - e_8 d_2; \quad e_1 = p_m R_k q_{m1} (C_{36}^k + C_{45}^k)$$

$$e_2 = p_m R_k [(C_{36}^k - C_{45}^k - C_{26}^k) + p_{m1} (C_{36}^k + C_{45}^k)]$$

$$e_3 = p_m R_k q_{m1} (C_{13}^k + C_{55}^k)$$

$$e_4 = p_m R_k [C_{13}^k - C_{12}^k + p_{m1} (C_{13}^k + C_{55}^k)]; \quad e_5 = C_{44}^k q_{m1} (2p_{m1} + 1)$$

$$e_6 = C_{44}^k (p_{m1}^2 - q_{m1}^2 + p_{m1}) - (C_{44}^k + p_m^2 R_k^2 C_{66}^k)$$

$$e_7 = 2C_{45}^k q_{m1} (p_{m1} + 1); \quad e_8 = C_{45}^k (p_{m1}^2 - q_{m1}^2 + 2p_{m1}) - p_m^2 R_k^2 C_{16}^k$$

$$d_1 = C_{33}^k q_{m1} (2p_{m1} + 1)$$

$$d_2 = C_{33}^k (p_{m1}^2 - q_{m1}^2 + p_{m1}) - (p_m^2 R_k^2 C_{55}^k + C_{22}^k)$$

$$d_3 = p_m R_k q_{m1} (C_{36}^k + C_{45}^k)$$

$$d_4 = p_m R_k [2C_{45}^k + C_{26}^k + p_{m1} (C_{36}^k + C_{45}^k)]$$

References

[1]Flugge, W., and Kelkar, V. S., "The Problem of an Elastic Circular Cylinder," *International Journal of Solids and Structures,* Vol. 4, No. 4, 1968, pp. 397–420.

[2]Yao, J. C., "Long Cylindrical Tube Subjected to Two Diametrically Opposite Loads," *The Aeronautical Quarterly,* Vol. 20, Nov.

1969, pp. 365–381.

[3]Srinivas, S.,"Analysis of Laminated Composite Circular Cylindrical Shells with General Boundary Conditions," NASA TR, R412, 1974.

[4]Varadan, T. K., and Bhaskar, K., "Bending of Laminated Orthotropic Cylindrical Shells—An Elasticity Approach," *Composite Structures,* Vol. 17, 1991, pp. 141–156.

[5]Pagano, N. J., "The Stress Field in a Cylindrically Anisotropic Body Under Two-Dimensional Surface Tractions," *Journal of Applied Mechanics,* Vol. 39, Sept. 1972, pp. 791–796.

[6]Ren, J. G., "Exact Solutions for Laminated Cylindrical Shells in Cylindrical Bending," *Composite Science and Technology,* Vol. 29, No. 3, 1987, pp. 169–187.

[7]Ren, J. G.,"Analysis of Simply-Supported Laminated Circular Cylindrical Shell Roofs," *Composite Structures,* Vol. 11, No. 4, 1989, pp. 277–292.

[8]Mikhailov, S. E., "General and Fundamental Solutions of Axisymmetric Torsion Equation for a Cylindrically Anisotropic Elastic Medium," *Mechanics of Composite,* Vol. 26, No. 3, 1991, pp. 52–55.

[9]Hyer, M. W., and Cooper, D. E., "Stresses and Deformations in Composite Tubes Due to a Circumferential Temperature Gradient," *Journal of Applied Mechanics,* Vol. 53, Dec. 1986, pp. 757–764.

[10]Kollar, L. P., Patterson, J. M., and Springer, G. S., "Composite Cylinders Subjected to Hygrothermal and Mechanical Loads," *International Journal of Solids and Structures,* Vol. 29, No. 12, 1992, pp. 1519–1534.

[11]Huang, N. N., and Tauchert, T. R., "Thermoelastic Solution for Cross-Ply Cylindrical Panels," *Journal of Thermal Stresses,* Vol. 14, No. 2, 1991, pp. 227–237.

[12]Huang, N. N., and Tauchert, T. R., "Thermal Stresses in Doubly-Curved Cross-Ply Laminates," *International Journal of Solids and Structures,* Vol. 29, No. 8, 1992, pp. 991–1000.

[13]Soong, T. V., "A Subdivisional Method for Linear System," *Proceedings of the 11th AIAA/ASME Structures, Structural Dynamics, and Materials Conferences,* AIAA, New York, 1970, pp. 211–223.

[14]Bhimaraddi, A., and Chandrashekhara, K., "Three-Dimensional Elasticity Solution for Static Response of Simply Supported Orthotropic Cylindrical Shells," *Composite Structures,* Vol. 20, No. 3, 1992, pp. 227–235.

[15]Wang, X., and Li, S. J., "Analytic Solution for Interlaminar Stresses in a Multilaminated Cylindrical Shell Under Thermal and Mechanical Loads," *International Journal of Solids and Structures,* Vol. 29, No. 10, 1992, pp. 1293–1302.

[16]Soldatos, K. P., and Hadjigeorgiou, V. P., "Three-Dimensional Solution of the Free Vibration Problem of Homogeneous Isotropic Cylindrical Shells and Panels," *Journal of Sound and Vibration,* Vol. 137, No. 3, 1990, pp. 369–384.

[17]Soldatos, K. P., "An Iterative Solution of a Bessel Equation Based on Torsional Vibrations of Orthotropic Hollow Cylinders," *Journal of Sound and Vibration,* Vol. 151, No. 1, 1991, pp. 149–152.

[18]Hawkes, T. D., and Soldatos, K. P., "Three-Dimensional Axisymmetric Vibrations of Orthotropic and Cross-Ply Laminated Hollow Cylinders," *AIAA Journal,* Vol. 30, No. 4, 1992, pp. 1089–1098.

[19]Bhimaraddi, A., "Free Vibration Analysis of Doubly Curved Shallow Shells on Rectangular Planform Using Three-Dimensional Elasticity Theory," *International Journal of Solids and Structures,* Vol. 27, No. 7, 1991, pp. 897–913.

[20]Chaudhuri, R. A., Balraman, K., and Kunukkasseril, X., "Arbitrarily Laminated, Anisotropic Cylindrical Shell Under Internal Pressure," *AIAA Journal,* Vol. 24, No. 11, 1986, pp. 1851–1858.

[21]Abu-Arija, K. R., and Chaudhuri, R. A., "Moderately Thick Angle-Ply Cylindrical Shells Under Internal Pressure," *Journal of Applied Mechanics,* Vol. 56, Sept. 1989, pp. 652–657.

[22]Seide, P., and Chaudhuri, R. A., "Triangular Finite Element for Analysis of Thick Laminated Shells," *International Journal for Numerical Methods in Engineering,* Vol. 24, Aug. 1987, pp. 1563–1579.

[23]Vinson, J. R., and Chou, T. W., *Composite Materials and Their Use in Structures,* Applied Science Publishers, London, England, UK, 1975.

[24]Pagano, N. J., and Whitney, J. M., "Geometric Design of Composite Cylindrical Characterization Specimens," *Journal of Composite Materials,* Vol. 4, July 1970, pp. 360–379.